

# Game-Theory-Assisted Reinforcement Learning for Border Defense: Early Termination based on Analytical Solutions

Goutam Das<sup>1</sup>, Michael Dorothy<sup>2</sup>, Kyle Volle<sup>3</sup>, and Daigo Shishika<sup>4</sup>

**Abstract**—Game theory provides the gold standard for analyzing adversarial engagements, offering strong optimality guarantees. However, these guarantees often become brittle when assumptions such as perfect information are violated. Reinforcement learning (RL), by contrast, is adaptive but can be sample-inefficient in large, complex domains. This paper introduces a hybrid approach that leverages game-theoretic insights to improve RL training efficiency. We study a border defense game with limited perceptual range, where defender performance depends on both search and pursuit strategies, making classical differential game solutions inapplicable. Our method employs the Apollonius Circle (AC) to compute equilibrium in the post-detection phase, enabling early termination of RL episodes without learning pursuit dynamics. This allows RL to concentrate on learning search strategies while guaranteeing optimal continuation after detection. Across single- and multi-defender settings, this early termination method yields 10–20% higher rewards, faster convergence, and more efficient search trajectories. Extensive experiments validate these findings and demonstrate the overall effectiveness of our approach.

## I. INTRODUCTION

Differential games model strategic interactions between competing agents in adversarial scenarios, initially formalized by Isaacs in his seminal work [1]. Border defense games [2]—also known as target defense [3], [4] or perimeter defense games [5]—represent a specialized variant where a team of defenders must protect a target region or boundary from infiltrating attackers [6], [7].

Analytical approaches yield exact solutions to these problems under simplifying assumptions on the dynamics, environments, and information structure. Isaacs established the relevance of Apollonius Circles (AC) for defining *dominance regions* in pursuit-evasion under simple motion, which was later formalized in [8]. Recent decomposition methods enable polynomial-time assignment algorithms for perimeter defense [9]–[12], with solutions for cooperative teams [13], [14], and heterogeneous attackers [15], [16].

However, analytical methods face fundamental limitations under partial information [17]–[19]. The stochastic nature of

the search problem under uncertainty about the attacker’s state makes it challenging to directly apply differential game techniques developed for full-state feedback settings. Moreover, standard decomposition into 1v1 or 2v1 subgames may overlook emergent cooperative behaviors.

Multi-agent reinforcement learning (MARL) methods such as MADDPG and MAPPO address partial observability and discover cooperative strategies without complete system models. Yet existing RL approaches learn both search and pursuit behaviors end-to-end, without leveraging available analytical solutions [20]. This results in sample inefficiency, requiring extensive computational resources to relearn known optimal capture strategies.

This paper presents a hybrid framework combining differential game theory with MARL for border defense under partial observability. Upon detecting the attacker, we use the Apollonius Circle to analytically compute the Nash equilibrium payoff of the resulting pursuit game, replacing simulation of the pursuit phase with this closed-form reward during RL training.

Our contributions are threefold:

- We present a novel hybrid framework that combines analytical game-theory (GT) solutions in the MARL training loop to improve learning efficiency,
- We empirically demonstrate that this approach achieves significantly higher rewards and faster convergence compared to end-to-end learning.
- We show that our method is effective across different team sizes, enabling the learning of robust search and coordination strategies.

**Paper Organization:** Section II formulates the two-phase border defense problem. Section III presents the Apollonius Circle method for Nash equilibrium computation. Section IV details the MARL formulation with GT-assisted early termination. Section V provides experimental evaluation using MAPPO. Section VI concludes with future directions.

## II. PROBLEM FORMULATION

We consider a target defense game in a bounded, two-dimensional environment,  $\Omega = [0, 1] \times [0, 1]$ . The game involves a team of  $n_d$  defenders,  $D_i$  for  $i \in \mathcal{I} = \{1, 2, \dots, n_d\}$ , and a single attacker,  $A$ . The defenders’ objective is to protect a target boundary,  $\mathcal{T}$ , located at the bottom edge of the environment, defined as  $\mathcal{T} = \{(x, y) \in \Omega \mid y = 0\}$ .

The state of the game at time  $t$  is given by  $\mathbf{x}(t) \triangleq [\mathbf{x}_{D_1}^\top(t), \dots, \mathbf{x}_{D_{n_d}}^\top(t), \mathbf{x}_A^\top(t)]^\top \in \mathbb{R}^{2(n_d+1)}$ , which concatenates the positions of all agents, where  $\mathbf{x}_k(t) = [x_k(t), y_k(t)]^\top$  denotes the position of agent  $k \in \{D_1, D_2, \dots, D_{n_d}, A\}$ . For notational brevity, we omit the

We gratefully acknowledge the support of ARL grant ARL DCIST CRA W911NF-17-2-0181 and AFRL grant FA8651-23-1-0012. The views expressed in this paper are those of the authors and do not reflect the official policy or position of the United States Government, Department of Defense, or its components.

<sup>1</sup>Goutam Das, Postdoctoral Researcher, School of Aeronautics and Astronautics, Purdue University, 610 Purdue Mall, West Lafayette, IN 47907, USA [das347@purdue.edu](mailto:das347@purdue.edu)

<sup>2</sup>Michael Dorothy, Army Research Directorate, DEVCOM Army Research Laboratory, APG, MD 21005, USA [michael.r.dorothy.civ@army.mil](mailto:michael.r.dorothy.civ@army.mil)

<sup>3</sup>Kyle Volle, is with the Munitions Directorate, Air Force Research Laboratory, Eglin AFB, FL 32542, USA [kyle@us.af.mil](mailto:kyle@us.af.mil).

<sup>4</sup>Daigo Shishika, Assistant Professor, Department of Mechanical Engineering, George Mason University, 4400 University Dr, Fairfax, VA 22030, USA [dshishik@gmu.edu](mailto:dshishik@gmu.edu)

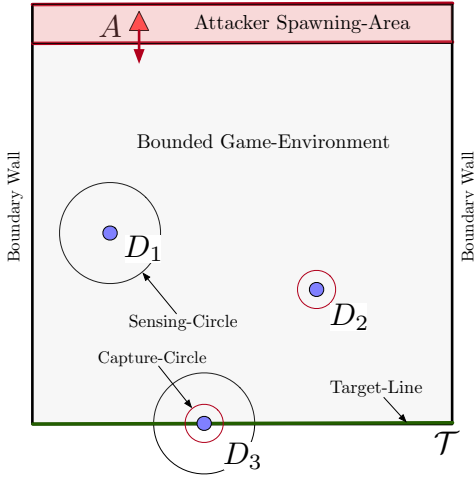


Fig. 1. Illustration of the border-defense game environment. An attacker ( $A$ ) spawns in the designated area at the top and attempts to reach the target line ( $\mathcal{T}$ ) at the bottom. The defender team, composed of agents with varying sensing ( $D_1, D_2$ ) and capture ( $D_2, D_3$ ) capabilities, must coordinate to intercept the attacker.

time argument ( $t$ ) when the context is clear. All agents are modeled with single-integrator dynamics:

$$\dot{\mathbf{x}}_k = v_k \mathbf{u}_k, \quad k \in \{D_1, \dots, D_{n_d}, A\}, \quad (1)$$

where  $v_k$  is the maximum speed of agent  $k$ , and  $\mathbf{u}_k$  is its control input, constrained to the set of admissible unit vectors,  $\mathcal{U} \triangleq \{\mathbf{u} \in \mathbb{R}^2 \mid \|\mathbf{u}\| \leq 1\}$ .

Each defender  $D_i$  is characterized by a sensing radius  $\rho_s^{(i)} \geq 0$  and a capture radius  $\rho_c^{(i)} \geq 0$ , as illustrated in Figure 1. We assume each defender is faster than the attacker, defining a speed ratio  $\nu_i = v_{D_i}/v_A > 1$  for all  $i \in \mathcal{I}$ , which is a necessary condition for capture.

The game begins under bilateral information asymmetry, with neither side having knowledge of the opponent's initial positions. Both the attacker's and the defenders' starting positions are drawn from uniform distributions over separate, predefined regions  $\Omega_A, \Omega_D \subset \Omega$ :

$$\mathbf{x}_A(0) \sim \text{Uniform}(\Omega_A), \quad (2)$$

$$\{\mathbf{x}_{D_i}(0)\}_{i \in \mathcal{I}} \sim \text{Uniform}(\Omega_D). \quad (3)$$

The game thus starts in a partial-information setting, which transitions to a perfect-information scenario when the attacker is sensed at  $t_s$ :

$$t_s = \inf\{t \geq 0 \mid \exists i \in \mathcal{I} \text{ s.t. } \|\mathbf{x}_A - \mathbf{x}_{D_i}\| \leq \rho_s^{(i)}\}. \quad (4)$$

We assume that, after sensing, full state information trivially becomes available to all agents for  $t \geq t_s$ .

We denote the defender and attacker policies as  $\gamma_{D_i}$  and  $\gamma_A$ , respectively. Prior to sensing ( $t < t_s$ ), each defender employs a policy based on the full-state information of all defenders:

$$\gamma_{D_i} : \mathcal{O}_i \rightarrow \mathcal{U}, \quad \text{for } i \in \mathcal{I}, \quad (5)$$

where  $\mathcal{O}_i$  represents the observation space of defender  $i$ , which includes its own position and the positions of other defenders. After sensing ( $t \geq t_s$ ), the defender policies have

access to the full state information:

$$\gamma_{D_i} : \mathbb{R}^{2(n_d+1)} \rightarrow \mathcal{U}. \quad (6)$$

Similarly, the attacker employs a two-stage policy:

$$\gamma_A = \begin{cases} \mathbf{u}_{\text{direct}} = [0, -1]^\top & \text{if } t < t_s, \\ \gamma_A^*(\mathbf{x}(t)) : \mathbb{R}^{2(n_d+1)} \rightarrow \mathcal{U} & \text{if } t \geq t_s, \end{cases} \quad (7)$$

where  $\mathbf{u}_{\text{direct}}$  denotes the attacker's fixed policy before sensing, and  $\gamma_A^*(\mathbf{x}(t))$  represents the attacker's optimal evasion strategy upon sensing. The direct-descent policy in Phase I is justified by the bilateral information asymmetry: since the attacker has no sensing capability and no knowledge of defender positions, any deviation from the shortest path to  $\mathcal{T}$  would only increase the time to reach the target without providing any informational benefit.

The game terminates at time  $t_f$  when the state  $\mathbf{x}(t_f)$  enters the terminal manifold  $\mathcal{S} = \mathcal{S}_A \cup \mathcal{S}_D$ , where:

$$\mathcal{S}_A = \{\mathbf{x} \mid y_A = 0\}, \quad (8a)$$

$$\mathcal{S}_D = \{\mathbf{x} \mid \exists i \in \mathcal{I} : \|\mathbf{x}_A - \mathbf{x}_{D_i}\| \leq \rho_c^{(i)}\}. \quad (8b)$$

The final time is thus  $t_f = \inf\{t \geq 0 \mid \mathbf{x}(t) \in \mathcal{S}\}$ .

This is a zero-sum game where the terminal payoff,  $J$ , is the attacker's distance from the target at the time of capture:

$$J = \max\{0, y_A(t_f)\}. \quad (9)$$

Given the uncertainty in the players' starting positions, the general zero-sum formulation is:

$$J^* = \max_{\gamma_D} \min_{\gamma_A} \mathbb{E}[J], \quad (10)$$

where  $\gamma_D = [\gamma_{D_1}, \gamma_{D_2}, \dots, \gamma_{D_{n_d}}]$  and the expectation is over initial conditions and any stochasticity in the policies. In this work, we fix the attacker policy as described in (7) and focus on learning the defender policy, reducing the problem to a one-sided optimization:

$$J^* = \max_{\gamma_D} \mathbb{E}[J \mid \gamma_A]. \quad (11)$$

### III. GAME THEORETIC ANALYSIS

We decompose the game into two phases based on available information and leverage the analytical solution of the second phase to develop GT-assisted early termination for RL.

#### A. Phase Decomposition and Strategic Coupling

The target defense game can be naturally divided into two sequential phases:

**Definition 1** (Phase I - Stochastic Search). *The search phase spans  $[0, t_s]$ , during which no defender has sensed the attacker (cf. (4)). Each defender's policy depends only on the positions of all defenders as defined in (5).*

**Definition 2** (Phase II - Deterministic Pursuit). *The pursuit phase begins at  $t_s$  when sensing occurs:*

$$\exists i \in \mathcal{I} : \|\mathbf{x}_A(t_s) - \mathbf{x}_{D_i}(t_s)\| = \rho_s^{(i)}. \quad (12)$$

For all  $t \geq t_s$ , defenders have access to the perfect state:

$$\mathcal{O}_i^H = \mathbf{x}(t) = [\mathbf{x}_{D_1}(t), \dots, \mathbf{x}_{D_{n_d}}(t), \mathbf{x}_A(t)]^\top. \quad (13)$$

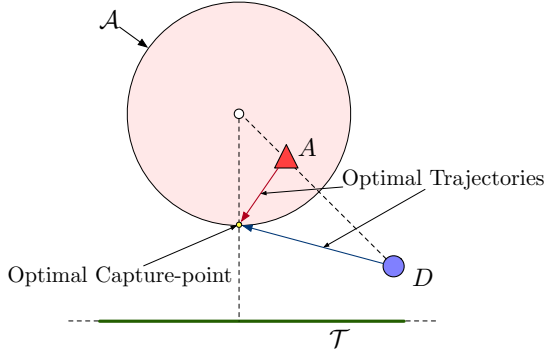


Fig. 2. Geometric representation of the optimal capture strategy in the deterministic pursuit phase (Phase II). The Apollonius Circle ( $\mathcal{A}$ ) defines the boundary of the attacker’s dominance region. The optimal capture point is the location on the circle with the minimum  $y$ -coordinate, and the optimal trajectories for both agents converge at this point.

Therefore, Phase I constitutes a stochastic optimization problem. In contrast, Phase II is a deterministic game of perfect information, for which an optimal defender policy can be derived. The full Phase I objective, formalized in Section III-C, is:

$$\gamma_D^{\text{I}^*} = \arg \max_{\gamma_D} \mathbb{E} [\mathbb{I}_{t_s < t_f} \cdot J^*(\mathbf{x}(t_s))], \quad (14)$$

where  $\mathbb{I}_{t_s < t_f}$  is the indicator function that equals 1 if sensing occurs before game termination and 0 otherwise, and the expectation is over initial conditions and policy stochasticity. Note that cases where sensing occurs but the defenders cannot prevent a breach are handled by  $J^*(\mathbf{x}(t_s)) = 0$ .

**Remark 1** (Search-Pursuit Trade-off). *The optimal Phase I policy must balance two competing objectives: maximizing the probability of sensing before game termination,  $\mathbb{P}[t_s < t_f]$ , through effective spatial coverage, and achieving a configuration  $\mathbf{x}(t_s)$  that maximizes the defender payoff. A myopic search strategy maximizing only sensing probability may result in poor pursuit configurations, yielding suboptimal overall performance despite successful sensing.*

### B. Analytical Solution for the Pursuit Phase

Once sensing occurs at time  $t_s$ , Phase II becomes a perfect information pursuit-evasion game. We leverage the geometric structure of the Apollonius Circle to compute the Nash equilibrium outcome analytically.

1) *Single Defender Case:* For a single defender-attacker pair with speed ratio  $\nu = v_D/v_A > 1$ , the Apollonius Circle  $\mathcal{A}(\mathbf{x}_A, \mathbf{x}_D, \nu)$  is the locus of points  $\mathbf{p}$  satisfying  $\|\mathbf{p} - \mathbf{x}_A\|/\|\mathbf{p} - \mathbf{x}_D\| = 1/\nu$ . The center  $\mathbf{c}$  and radius  $r$  of  $\mathcal{A}$  are given by:

$$\mathbf{c} = \frac{\nu^2 \mathbf{x}_A - \mathbf{x}_D}{\nu^2 - 1}, \quad (15a)$$

$$r = \frac{\nu \|\mathbf{x}_A - \mathbf{x}_D\|}{|\nu^2 - 1|}. \quad (15b)$$

**Lemma 1** (Dominance Region [1], [8]). *The closed disk  $\mathcal{D}(\mathbf{x}_A, \mathbf{x}_D, \nu_i) = \{\mathbf{p} : \|\mathbf{p} - \mathbf{c}_i\| \leq r_i\}$  is the attacker’s dominance region—the set of points the attacker can reach no later than the defender.*

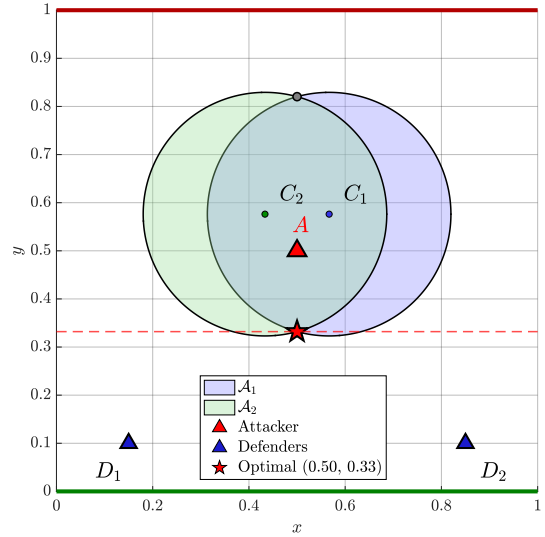


Fig. 3. Optimal capture point computation for a multi-defender scenario. The attacker’s reachable region is the intersection of the individual Apollonius Circles ( $\mathcal{A}_1, \mathcal{A}_2$ ). The optimal interception point, marked by the red star, corresponds to the minimum  $y$ -coordinate within this intersection, representing the game-theoretic payoff.

**Theorem 1** (Nash Equilibrium Payoff). *For the Phase II pursuit game starting at configuration  $\mathbf{x}(t_s)$ , the Nash equilibrium payoff is:*

$$J^*(\mathbf{x}(t_s)) = \max\{0, c_y - r\}, \quad (16)$$

where  $c_y$  is the  $y$ -coordinate of the Apollonius Circle center and  $r$  is its radius.

*Proof.* The result follows from Lemma 1: the attacker’s optimal strategy is to move toward the lowest point of the dominance region,  $\mathbf{p}^* = [c_x, c_y - r]^T$ , while the defender moves to intercept at  $\mathbf{p}^*$ . The payoff is clamped at 0 when  $c_y - r < 0$ , indicating the attacker reaches  $\mathcal{T}$  before interception.  $\square$

**Remark 2** (Effect of Nonzero Capture Radius). *The Nash payoff in (16) assumes point capture ( $\rho_c = 0$ ). When  $\rho_c > 0$ , the defender can intercept the attacker once  $\|\mathbf{x}_A - \mathbf{x}_D\| \leq \rho_c$ , allowing capture to occur before the agents reach the point-capture meeting location predicted by the Apollonius Circle analysis. Consequently, (16) provides a conservative approximation of the true Phase II payoff when  $\rho_c > 0$ .*

2) *Multiple Defender Case:* For multiple defenders with capture capabilities, the attacker’s dominance region becomes the intersection of individual Apollonius Circles.

**Definition 3** (Multi-Defender Dominance Region). *Given  $n_c$  defenders with capture capability at positions  $\{\mathbf{x}_{D_i}\}_{i \in \mathcal{I}_c}$  and speed ratios  $\{\nu_i\}_{i \in \mathcal{I}_c}$ , the attacker’s dominance region is:*

$$\mathcal{R}_A = \bigcap_{i \in \mathcal{I}_c} \mathcal{D}(\mathbf{x}_A, \mathbf{x}_{D_i}, \nu_i). \quad (17)$$

Figure 3 illustrates this geometric relationship for a two-defender scenario, showing how the optimal capture point corresponds to the minimum  $y$ -coordinate within the intersection region.

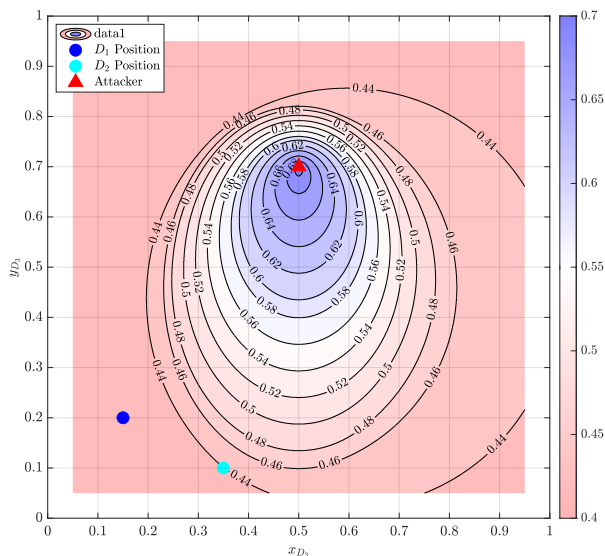


Fig. 4. Value function level-set for optimal defender placement. The contours illustrate the Nash equilibrium payoff ( $J^*$ ) as a function of a third defender's position, given two fixed defenders. Blue regions indicate configurations that yield a better payoff for the attacker, while red regions are more favorable for the defenders.

**Proposition 1 (Multi-Defender Nash Equilibrium).** *For multiple defenders, the Nash equilibrium payoff is:*

$$J^*(\mathbf{x}(t_s)) = \min_{\mathbf{p} \in \text{cl}(\mathcal{R}_A)} p_y. \quad (18)$$

The computation of (18) requires solving a constrained optimization problem:

$$\min_{\mathbf{p}: p_y} p_y \quad (19)$$

$$\text{s.t. } \|\mathbf{p} - \mathbf{c}_i\|^2 \leq r_i^2, \quad \forall i \in \mathcal{I}_c, \quad (20)$$

where  $\mathbf{c}_i$  and  $r_i$  are the center and radius of the  $i$ -th Apollonius Circle.

Figure 4 demonstrates how the Nash equilibrium payoff varies with defender positioning, illustrating the importance of spatial configuration quality during the search phase.

**Remark 3 (Computational Complexity).** *While the single-defender case admits a closed-form solution, the multi-defender case requires numerical optimization. However, the problem remains convex (minimizing a linear objective over an intersection of convex sets), ensuring efficient computation via standard convex optimization techniques.*

### C. GT-Assisted Reward Mechanism

The analytical solution for Phase II enables a training approach that eliminates the need to learn pursuit dynamics while maintaining theoretical optimality. Crucially, RL remains essential for learning the Phase I search strategies, for which no analytical solution exists. We formalize this mechanism and establish its relationship to full trajectory simulation.

1) *Early Termination Principle:* Traditional reinforcement learning for target defense requires agents to learn both search and pursuit behaviors through extensive trial and error. Our GT-assisted approach leverages the analytical solu-

tion from Section III-B to provide immediate, theoretically-grounded rewards at sensing time.

**Definition 4 (GT-Assisted Termination).** *Upon sensing at time  $t_s$  with configuration  $\mathbf{x}(t_s)$ , the GT-assisted mechanism:*

- 1) *Computes the Nash equilibrium payoff  $J^*(\mathbf{x}(t_s))$  using equation (18)*
- 2) *Terminates the episode immediately*
- 3) *Assigns terminal reward  $R = J^*(\mathbf{x}(t_s))$  to all defenders*

This approach contrasts with standard RL training requiring agents to learn pursuit strategies through exploration.

2) *Undiscounted Payoff Equivalence:* Let  $R^{\text{GT}}$  and  $R^{\text{full}}$  denote the rewards from GT-assisted termination and full optimal pursuit simulation, respectively. Then:

$$R^{\text{GT}}(\mathbf{x}(t_s)) = \mathbb{E}[R^{\text{full}}(\mathbf{x}(t_s)) | \text{optimal play}]. \quad (21)$$

By Theorem 1, the GT-assisted mechanism assigns:

$$R^{\text{GT}}(\mathbf{x}(t_s)) = J^*(\mathbf{x}(t_s)), \quad (22)$$

which equals  $y_A(t_f^*)$  under optimal play by both sides, where  $t_f^*$  is the optimal termination time. Note that while the undiscounted terminal payoffs are equivalent, the discounted returns generally differ because the GT-assisted reward is assigned at  $t_s < T_f$ . Thus, under discounting, the GT-assisted formulation induces a modified learning objective that places additional value on earlier sensing, which is aligned with our goal of encouraging efficient search behavior. For suboptimal play, the GT-assisted reward provides an upper bound, preventing reward exploitation through poor pursuit execution.

3) *Computational and Learning Advantages:* The GT-assisted mechanism provides several key advantages:

**Proposition 2 (Computational Efficiency).** *The GT-assisted approach reduces the computational cost of each episode by eliminating the simulation of the pursuit phase. The number of saved steps per episode,  $T_p$ , can be estimated by considering a direct, one-dimensional pursuit:*

$$T_p \approx \frac{(\rho_s - \rho_c)/(v_D - v_A)}{\Delta t} \quad (23)$$

where the numerator represents the approximate time required to close the distance from sensing to capture at the maximum relative speed, and the denominator converts this time into discrete simulation steps.

This shorter horizon also improves sample efficiency by removing the need to explore pursuit strategies.

4) *Impact on Learned Behaviors:* The GT-assisted mechanism shapes the learned search strategies through the objective defined in (14): the policy must learn to position defenders not just for sensing, but for configurations that enable effective pursuit—despite never experiencing pursuit during training.

## IV. MULTI-AGENT REINFORCEMENT LEARNING APPROACH

### A. Decentralized Partially Observable MDP Formulation

We formulate the problem as a Decentralized Partially Observable Markov Decision Process (Dec-POMDP) defined by

---

**Algorithm 1** GT-Assisted Episode Termination
 

---

```

1: Input: Sensing configuration  $\mathbf{x}(t_s)$ , speed ratios  $\{\nu_i\}$ 
2: Output: Terminal reward  $R$ 
3: // Extract positions
4:  $\mathbf{x}_A \leftarrow \text{AttackerPosition}(\mathbf{x}(t_s))$ 
5:  $\{\mathbf{x}_{D_i}\} \leftarrow \text{DefenderPositions}(\mathbf{x}(t_s))$ 
6: // Compute Apollonius Circles
7: for each defender  $i$  with capture capability do
8:    $\mathbf{c}_i \leftarrow (\nu_i^2 \mathbf{x}_A - \mathbf{x}_{D_i}) / (\nu_i^2 - 1)$ 
9:    $r_i \leftarrow \nu_i \|\mathbf{x}_A - \mathbf{x}_{D_i}\| / |\nu_i^2 - 1|$ 
10: end for
11: // Solve for Nash equilibrium
12: if single defender then
13:    $J^* \leftarrow \max\{0, c_y - r\}$ 
14: else
15:    $J^* \leftarrow \text{SolveConvexOptimization}(\{\mathbf{c}_i, r_i\})$ 
16: end if
17: return  $R = J^*$ 

```

---

the tuple:

$$\{\mathcal{I}, \mathcal{S}, \{\mathcal{A}_i\}_{i \in \mathcal{I}}, \{\mathcal{O}_i\}_{i \in \mathcal{I}}, T, \{R_i\}_{i \in \mathcal{I}}, \gamma\}, \quad (24)$$

where:

- $\mathcal{I} = \{1, 2, \dots, n_d\}$ : defender index set;
- $\mathcal{S} = \Omega^{n_d+1} \subset \mathbb{R}^{2(n_d+1)}$ : global state space with  $\mathbf{s}_t \equiv \mathbf{x}(t)$ ;
- $\mathcal{A}_i \subset \mathbb{R}$ : action space for defender  $i$ ;
- $\mathcal{O}_i$ : phase-dependent observation space as defined in Section II;
- $T : \mathcal{S} \times \mathcal{A}_1 \times \dots \times \mathcal{A}_{n_d} \rightarrow \Delta(\mathcal{S})$ : transition function governed by (1) and (7);
- $R_i : \mathcal{S} \rightarrow \mathbb{R}$ : reward function for defender  $i$ ;
- $\gamma \in [0, 1)$ : discount factor.

Each defender  $i$  learns a policy  $\pi_{\theta_i} : \mathcal{O}_i \rightarrow \Delta(\mathcal{A}_i)$ , corresponding to the strategy  $\gamma_{D_i}$  from Section II. The team objective is to learn a joint policy  $\boldsymbol{\pi}_{\theta} = \{\pi_{\theta_1}, \dots, \pi_{\theta_{n_d}}\}$  maximizing the expected cumulative discounted reward:

$$J(\boldsymbol{\theta}) = \mathbb{E}_{\boldsymbol{\pi}_{\theta}} \left[ \sum_{t=0}^{T_f} \gamma^t R_t \mid \mathbf{s}_0 \sim \rho_0 \right], \quad (25)$$

where  $T_f$  is the episode termination time,  $R_t$  is the shared team reward at time  $t$ , and  $\rho_0$  represents the initial state distribution defined by (2)–(3). We note that the learned policies are not guaranteed to converge to a global optimum, nor are they directly interpretable; however, the GT-assisted reward mechanism ensures that the pursuit phase outcome is always evaluated optimally.

### B. Observation and Action Spaces

1) *Action Space*: Each defender  $i$  controls its heading through a continuous action:

$$a_t^i \in \mathcal{A}_i = [-1, 1] \subset \mathbb{R}, \quad (26)$$

mapping to the control input  $\mathbf{u}_{D_i}(t)$  in (1) via:

$$\mathbf{u}_{D_i}(t) = \begin{bmatrix} \cos(a_t^i \cdot \pi) \\ \sin(a_t^i \cdot \pi) \end{bmatrix}, \quad (27)$$

ensuring  $\|\mathbf{u}_{D_i}(t)\| = 1$  as required by the dynamics.

2) *Phase-Dependent Observations*: The information asymmetry at sensing time  $t_s$  induces phase-dependent observation spaces for each defender.

**Phase I (Search Phase,  $t < t_s$ ):** Before sensing, defender  $i$  observes its own position and those of teammate defenders:

$$\mathbf{o}_t^i \in \mathcal{O}_i^I \subset \mathbb{R}^{2n_d}, \quad (28)$$

where

$$\mathbf{o}_t^i = [\mathbf{x}_{D_1}^\top(t), \dots, \mathbf{x}_{D_{n_d}}^\top(t)]^\top. \quad (29)$$

The attacker position  $\mathbf{x}_A(t)$  is not observable during this phase. Defenders share their positions via communication, so the partial observability is solely due to the unknown attacker state.

**Phase II (Pursuit Phase,  $t \geq t_s$ ):** Upon sensing, the attacker's position becomes observable to all defenders:

$$\mathbf{o}_t^i \in \mathcal{O}_i^{\text{II}} = \Omega^{n_d+1} \subset \mathbb{R}^{2(n_d+1)}, \quad (30)$$

where

$$\mathbf{o}_t^i = [\mathbf{x}_{D_1}^\top(t), \dots, \mathbf{x}_{D_{n_d}}^\top(t), \mathbf{x}_A^\top(t)]^\top = \mathbf{s}_t. \quad (31)$$

Pursuers with  $\rho_s^{(i)} = 0$  also gain access to the full state once any sensor detects the attacker.

### C. Reward Structure and Terminal Conditions

We evaluate two reward structures that differ in their terminal conditions and reward assignment mechanisms, enabling a comparative analysis of GT-assisted early termination versus standard end-to-end learning.

1) *GT-Assisted Reward*: In the GT-assisted approach, episodes terminate immediately upon sensing at time  $t_s$ , and the terminal reward is computed using the Nash equilibrium payoff from (18):

$$R_t^i = \begin{cases} 0 & \text{if } t < t_s, \\ J^*(\mathbf{x}(t_s)) & \text{if } t = t_s, \end{cases} \quad \forall i \in \mathcal{I}, \quad (32)$$

where  $J^*(\mathbf{x}(t_s))$  is the analytically computed Nash equilibrium payoff given by (16) for a single defender or (18) for multiple defenders. The terminal condition is:

$$\mathcal{S}_{\text{term}}^{\text{GT}} = \{\mathbf{s}_t \in \mathcal{S} \mid \exists i \in \mathcal{I} : \|\mathbf{x}_A(t) - \mathbf{x}_{D_i}(t)\| \leq \rho_s^{(i)}\}. \quad (33)$$

From (22), this reward is equivalent to the expected outcome under optimal play in Phase II, eliminating the need for defenders to learn pursuit dynamics while providing theoretically grounded feedback for search strategy optimization.

2) *Standard Reward*: In the standard approach, episodes continue through both search and pursuit phases until either capture or target breach occurs. The terminal reward is:

$$R_t^i = \begin{cases} 0 & \text{if } t < T_f, \\ \max\{0, y_A(T_f)\} & \text{if } t = T_f, \end{cases} \quad \forall i \in \mathcal{I}, \quad (34)$$

where  $T_f$  is the episode termination time and  $y_A(T_f)$  is the attacker's final  $y$ -coordinate. The terminal condition is:

$$\mathcal{S}_{\text{term}}^{\text{std}} = \{\mathbf{s}_t \in \mathcal{S} \mid y_A(t) \leq 0 \text{ or } \exists i \in \mathcal{I}_c : \|\mathbf{x}_A(t) - \mathbf{x}_{D_i}(t)\| \leq \rho_c^{(i)}\}, \quad (35)$$

where  $\mathcal{I}_c = \{i \in \mathcal{I} \mid \rho_c^{(i)} > 0\}$  is the set of defenders with capture capability.

3) *Shared Reward Structure*: In both approaches, all defenders receive identical rewards ( $R_t^i = R_t$  for all  $i \in \mathcal{I}$ ) to encourage cooperative behavior and team coordination. This shared reward structure is critical for learning coordinated search patterns in Phase I. While individual reward schemes could reduce credit misattribution for a single agent’s actions, they risk incentivizing greedy behaviors that undermine team coordination—particularly in the heterogeneous setting where the sensor’s contribution is only realized through the pursuer’s capture. The shared structure ensures all agents are aligned toward the common team objective.

#### D. Multi-Agent Proximal Policy Optimization

We employ MAPPO [21] via the BenchMARL framework [22], which extends PPO to multi-agent settings through centralized training with decentralized execution (CTDE).

1) *Policy and Value Networks*: Each defender  $i$  maintains a policy network  $\pi_{\theta_i} : \mathcal{O}_i \rightarrow \Delta(\mathcal{A}_i)$  outputting a Gaussian distribution:

$$a_t^i \sim \mathcal{N}(\mu_{\theta_i}(\mathbf{o}_t^i), \sigma_{\theta_i}(\mathbf{o}_t^i)), \quad (36)$$

where  $\mu_{\theta_i}$  and  $\sigma_{\theta_i}$  are the mean and standard deviation networks, with sampled actions clamped to  $[-1, 1]$ . A centralized critic  $V_\phi : \mathcal{S} \rightarrow \mathbb{R}$  estimates the state value using global information during training:

$$V_\phi(\mathbf{s}_t) \approx \mathbb{E} \left[ \sum_{k=t}^{T_f} \gamma^{k-t} R_k \mid \mathbf{s}_t \right], \quad (37)$$

where  $R_k$  denotes the shared team reward at time  $k$  (as all defenders receive identical rewards).

At execution time, each defender acts based only on local observations  $\mathbf{o}_t^i$ , enabling decentralized execution.

2) *Training Objective*: Each policy is updated by maximizing the clipped surrogate objective:

$$L^{\text{CLIP}}(\theta_i) = \mathbb{E}_t \left[ \min \left( r_t^i(\theta_i) \hat{A}_t^i, \text{clip}(r_t^i(\theta_i), 1 - \epsilon, 1 + \epsilon) \hat{A}_t^i \right) \right], \quad (38)$$

where  $r_t^i(\theta_i) = \pi_{\theta_i}(a_t^i | \mathbf{o}_t^i) / \pi_{\theta_i^{\text{old}}}(a_t^i | \mathbf{o}_t^i)$  is the probability ratio,  $\epsilon$  is the clip parameter, and  $\hat{A}_t^i$  is computed via GAE [23]:

$$\hat{A}_t^i = \sum_{l=0}^{\infty} (\gamma \lambda)^l \delta_{t+l}, \quad (39)$$

with  $\delta_t = R_t + \gamma V_\phi(\mathbf{s}_{t+1}) - V_\phi(\mathbf{s}_t)$  being the temporal difference error.

## V. EXPERIMENTS

Experiments<sup>1</sup> used BenchMARL [22] with VMAS [24] for vectorized simulation, employing MAPPO with 20 parallel environments, training for 1.2–1.8M frames over 3 seeds. Table I summarizes the environment parameters. Homogeneous defender team was tested with the sensing radius  $\rho_s = 0.3$  for 1v1 (1 defender, 1 attacker) and  $\rho_s = 0.15$  for 3v1 (3 defenders, 1 attacker) and the capture radius of  $\rho_c = 0.07$ .

<sup>1</sup>Code and experimental data are available at <https://github.com/das-goutam/benchmarl-target-defense>

TABLE I  
ENVIRONMENT PARAMETERS

Parameter	Value
Domain	$\Omega = [0, 1] \times [0, 1]$
Target boundary	$\mathcal{T} = \{(x, y) \in \Omega \mid y = 0\}$
Attacker spawn region	$\Omega_A = [0, 1] \times [0.9, 1.0]$
Speed ratio	$\nu = v_{D_i} / v_A = 3.33$
Sensing radius	$\rho_s \in \{0.15, 0.3, 0.35\}$
Capture radius	$\rho_c = 0.07$
Time step	$\Delta t = 0.05$
Max episode length	$T_{\max} = 2 / (v_A \Delta t)$ steps

#### A. Team Performance

In scenarios with homogeneous defenders, the GT-assisted approach consistently outperforms the end-to-end baseline in both single-defender (1v1) and multi-defender (3v1) configurations (Figs. 5 & 6, respectively). For the 1v1 case, the GT-assisted policy converges rapidly to a mean reward of  $\mu = 0.605$ , a 10% improvement over the baseline’s  $\mu = 0.545$ . This advantage is maintained in the 3v1 setting, where the GT-assisted method achieves a final reward of  $\mu = 0.745$ , representing a 18.9% increase over the baseline’s  $\mu = 0.626$ . While the end-to-end approach could in principle converge to similar performance given sufficient training, it must simultaneously learn both search and pursuit behaviors, resulting in a fundamentally larger exploration space that hinders convergence in practice.

#### B. Spatial Configuration Quality Analysis

To evaluate whether GT-assisted training produces superior spatial configurations at sensing, we analyze the Nash equilibrium payoffs  $J^*(\mathbf{x}(t_s))$  computed at sensing time for both approaches across 1,000 evaluation episodes in a homogeneous 3v1 environment with sensing radius  $\rho_s = 0.15$  and speed ratio  $\nu = 3.33$ .

Figure 7 presents the comparison between the two scenarios. In particular, Figure 7(c) reveals that GT-assisted training achieves higher Nash payoffs in successfully sensed episodes, with a median value of 0.768 versus 0.701 for

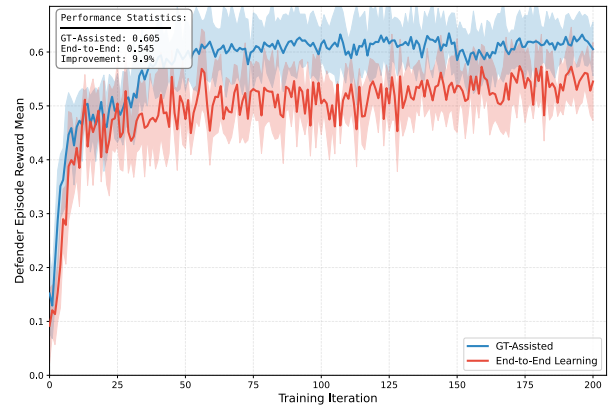


Fig. 5. Training performance in the 1v1 homogeneous scenario. The GT-assisted policy (blue) converges faster and to a significantly higher mean reward ( $\mu = 0.605$ ) than the end-to-end baseline (red,  $\mu = 0.545$ ), demonstrating a 10% performance improvement.

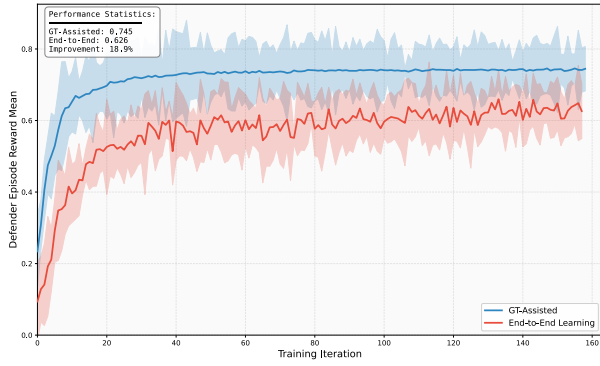


Fig. 6. Training performance in the 3v1 homogeneous scenario. The GT-assisted approach (blue) again shows superior performance, achieving a stable mean reward of  $\mu = 0.745$  with lower variance. The end-to-end method (red) converges to a lower reward of  $\mu = 0.626$ .

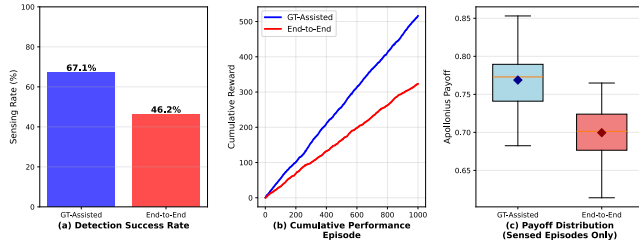


Fig. 7. Evaluation of spatial configuration quality for the 3v1 homogeneous scenario ( $\rho_s = 0.15$ ) over 1,000 test episodes. (a) The GT-assisted policy achieves a much higher sensing rate (67.1%) compared to the baseline (45.2%). (b) This leads to superior cumulative performance. (c) For episodes where sensing occurred, the GT-assisted policy achieves a distribution of Apollonius payoffs with a significantly higher median (0.768 vs. 0.701), indicating that it learns to position defenders more strategically at the moment of sensing.

end-to-end learning, which suggests better defender spatial configuration under GT-assisted training.

## VI. CONCLUSION

This paper presents a hybrid framework that integrates game-theoretic analytical solutions with multi-agent reinforcement learning for a border defense game. By computing Nash equilibrium payoffs analytically at the moment of sensing, our approach eliminates the need to learn deterministic pursuit dynamics and concentrates computational resources on the challenging stochastic search problem.

Experimental evaluation across homogeneous defender teams demonstrates that GT-assisted early termination achieves superior performance compared to standard end-to-end learning, with faster convergence rates and better strategic spatial configurations at sensing time. Future work will extend this hybrid approach to scenarios with multiple simultaneous attackers, which would require handling partial sensing transitions as not all attackers may be detected at the same time, and investigate scalability to larger teams where the convex optimization for Apollonius Circle intersections may become more demanding. Incorporating additional game-theoretic insights into the search phase to further improve sample efficiency and coordination quality is also a promising direction.

## REFERENCES

- [1] R. Isaacs, *Differential Games: A Mathematical Theory with Applications to Optimization, Control and Warfare*. Wiley, New York, 1965.
- [2] A. Von Moll, E. Garcia, D. Casbeer, M. Suresh, and S. C. Swar, "Multiple-pursuer, single-evader border defense differential game," *Journ. of Aerospace Info. Syst.*, vol. 17, no. 8, pp. 407–416, 2020.
- [3] E. Garcia, D. W. Casbeer, and M. Pachter, "Active target defense using first order missile models," *Automatica*, vol. 78, pp. 139–143, 2017.
- [4] H. Fu and H. H.-T. Liu, "Guarding a territory against an intelligent intruder: Strategy design and experimental verification," *IEEE/ASME Transactions on Mechatronics*, vol. 25, no. 4, pp. 1765–1772, 2020.
- [5] D. Shishika and V. Kumar, "Perimeter-defense game on arbitrary convex shapes," *arXiv preprint arXiv:1909.03989*, 2019.
- [6] I. E. Weintraub, M. Pachter, and E. Garcia, "An introduction to pursuit-evasion differential games," in *2020 American Control Conf. (ACC)*. IEEE, 2020, pp. 1049–1066.
- [7] D. Shishika, J. Paulos, and V. Kumar, "Cooperative team strategies for multi-player perimeter-defense games," *IEEE Robotics and Automation Lett.*, vol. 5, no. 2, pp. 2738–2745, 2020.
- [8] M. Dorothy, D. Maity, D. Shishika, and A. Von Moll, "One apollonius circle is enough for many pursuit-evasion games," *Automatica*, vol. 163, p. 111587, 2024.
- [9] D. Shishika and V. Kumar, "Local-game decomposition for multiplayer perimeter-defense problem," in *2018 IEEE Conf. on Decision and Control (CDC)*, 2018, pp. 2093–2100.
- [10] E. Garcia, D. W. Casbeer, A. Von Moll, and M. Pachter, "Multiple pursuer multiple evader differential games," *IEEE Trans. on Automatic Control*, vol. 66, no. 5, pp. 2345–2350, 2021.
- [11] S. Bajaj, E. Torng, S. D. Bopardikar, A. Von Moll, I. Weintraub, E. Garcia, and D. W. Casbeer, "Competitive perimeter defense of conical environments," *2022 IEEE 61st Conference on Decision and Control (CDC)*, pp. 6586–6593, 2022.
- [12] R. Yan, Z. Shi, and Y. Zhong, "Task assignment for multiplayer reach-avoid games in convex domains via analytical barriers," *IEEE Transactions on Robotics*, vol. 36, no. 1, pp. 107–124, 2019.
- [13] D. Milutinović, A. Von Moll, S. G. Manyam, D. W. Casbeer, I. E. Weintraub, and M. Pachter, "Cooperative pursuit-evasion games with a flat sphere condition," *IEEE Open Journal of Control Systems*, 2025.
- [14] Z. E. Fuchs, P. P. Khargonekar, and J. Evers, "Cooperative defense within a single-pursuer, two-evader pursuit evasion differential game," in *49th IEEE conference on decision and control (CDC)*. IEEE, 2010, pp. 3091–3097.
- [15] Y. Lee, G. Das, D. Shishika, and E. Bakolas, "Guarding a target area from a heterogeneous group of cooperative attackers," in *2024 American Control Conference (ACC)*. IEEE, 2024, pp. 233–238.
- [16] G. Das, V. Rostobaya, J. Berneburg, Z. I. Bell, M. Dorothy, and D. Shishika, "Heterogeneous roles against assignment based policies in two vs two target defense game," in *2024 IEEE 63rd Conference on Decision and Control (CDC)*. IEEE, 2024, pp. 8416–8422.
- [17] D. Shishika, D. Maity, and M. Dorothy, "Partial info. target defense game," in *2021 IEEE Inter. Conf. on Robotics and Automation (ICRA)*. IEEE, 2021, pp. 8111–8117.
- [18] D. Maity and A. Pourghorban, "Cooperative target defense under communication and sensing constraints," *IEEE Control Systems Letters*, 2024.
- [19] S. D. Bopardikar, F. Bullo, and J. P. Hespanha, "On discrete-time pursuit-evasion games with sensing limitations," *IEEE Transactions on Robotics*, vol. 24, no. 6, pp. 1429–1439, 2008.
- [20] Y. Wang, L. Dong, and C. Sun, "Cooperative control for multi-player pursuit-evasion games with reinforcement learning," *Neurocomputing*, vol. 412, pp. 101–114, 2020.
- [21] C. Yu, A. Velu, E. Vinitzky, J. Gao, Y. Wang, A. Bayen, and Y. Wu, "The surprising effectiveness of ppo in cooperative multi-agent games," *Advances in neural information processing systems*, vol. 35, pp. 24 611–24 624, 2022.
- [22] M. Bettini, A. Prorok, and V. Moens, "Benchmark! Benchmarking multi-agent reinforcement learning," *Journal of Machine Learning Research*, vol. 25, no. 217, pp. 1–10, 2024.
- [23] J. Schulman, P. Moritz, S. Levine, M. Jordan, and P. Abbeel, "High-dimensional continuous control using generalized advantage estimation," *arXiv preprint arXiv:1506.02438*, 2015.
- [24] M. Bettini, R. Kortvelesy, J. Blumenkamp, and A. Prorok, "Vmas: A vectorized multi-agent simulator for collective robot learning," in *International Symposium on Distributed Autonomous Robotic Systems*. Springer, 2022, pp. 42–56.